4DATLANTIC-OHC

ALGORITHM THEORETICAL BASIS DOCUMENT

	Name	Organisation	Date	Visa
Written by:	Michaël Ablain Robin Fraudeau Florence Marti Ramiro Ferrari	Magellium	15/12/2024	
Checked by:	Michaël Ablain	Magellium	15/12/2024	
Approved by:	Gilles Larnicol	Magellium	15/12/2024	
Accepted by:	Roberto Sabia	ESA	15/12/2024	

Document reference:	OHCATL-DT-020-MAG_ATBD
Edition.Revision:	2.0
Date Issued:	15/12/2024
Customer :	ESA
Ref. Market, consultation :	AO/1-10546/20/I-NB
Contrat No. :	4000134928/21/I-NB

Distribution List

	Name	Organisation	Nb. copies
Sent to :	Roberto Sabia	ESA	1 (digital copy)
Internal copy :	Project Report	Magellium	1 (digital copy)

Document evolution sheet

Ed.	Rev.	Date	Purpose evolution	Comments
1	0	02/02/2022	Creation of document	
1	1	15/06/2022	Minor modifications due to ESA feedbacks	
1	2	17/08/2022	Minor modifications	Introduction section 2 - Sections 2.1, 3.5.2, 4.4.6, 5.4.3
2	0	15/12/2024	Modifications related to version 2.0 of the product	

Contents

This document is property of Magellium. It cannot be reproduced, nor communicated without permission.

page 4/37

List of figures

List of tables

This document is property of Magellium. It cannot be reproduced, nor communicated without permission.

page 5/37

1. Introduction

1.1. Executive summary

Given the major role of the Atlantic Ocean in the climate system, it is essential to characterise the temporal and spatial variations of its heat content. The 4DAtlantic Project (https://eo4society.esa.int/projects/4datlantic-ohc/) aims at developing and testing space geodetic methods to estimate the regional **ocean heat content** (OHC) change over the Atlantic Ocean from satellite altimetry and gravimetry. The strategy developed in the frame of the ESA MOHeaCAN Project (https://eo4society.esa.int/projects/moheacan/) is pursued and refined at spatial regional scales both for the data generation and the uncertainty estimate. At two test sites, OHC change derived from in situ data (RAPID and OVIDE-AR7W) are used to evaluate the accuracy and reliability of the new space geodetic based OHC change. The Atlantic OHC product will be used to better understand the complexity of the Earth's climate system. In particular, the project aims at better understanding the role played by the Atlantic Meridional Overturning Circulation (AMOC) in regional and global climate change, and the variability of the Meridional Heat transport in the North Atlantic. In addition, improving our knowledge on the Atlantic OHC change will help to better assess the global ocean heat uptake and thus estimate the Earth's energy imbalance more accurately as the ocean absorbs about 90% of the excess energy stored by the Earth system.

In the 4DAtlantic project, the OHC change is estimated from the measurement of the thermal expansion of the ocean. The latter is obtained by removing the ocean mass change and the sea level change due to salinity (halosteric sea level changes) derived from gravimetry and in situ data respectively to the total sea-level change derived from altimetry measurements. This approach provides consistent spatial and temporal sampling of the ocean heat content change in the Atlantic Ocean.

4DAtlantic project's objectives are to develop novel algorithms, estimate realistic regional OHC uncertainties thanks to a rigorous error budget of the altimetric, gravimetric and in-situ instruments in order to reach the challenging target for the uncertainty quantification.

1.2. Scope and objectives

This document is the Algorithm Theoretical Basis Document (ATBD) of the 4DAtlantic OHC product supported by ESA. This ATBD is dedicated to the description and justification of the algorithms used in the generation of the **OHC change**.

The calculation of the 4DAtlantic OHC product is divided in several steps as presented in the following figure (Figure 1). The first step is to process the input data from the altimetry, gravimetry and in-situ measurements to allow their differences to be calculated in the next step. Then the processing of the OHC at spatial regional scales can be carried out. The last step consists in computing uncertainties of the 4DAtlantic OHC product, propagating the uncertainties at spatial regional scales from input data until the final product.

This document is property of Magellium. It cannot be reproduced,nor communicated without permission.

page 6/37
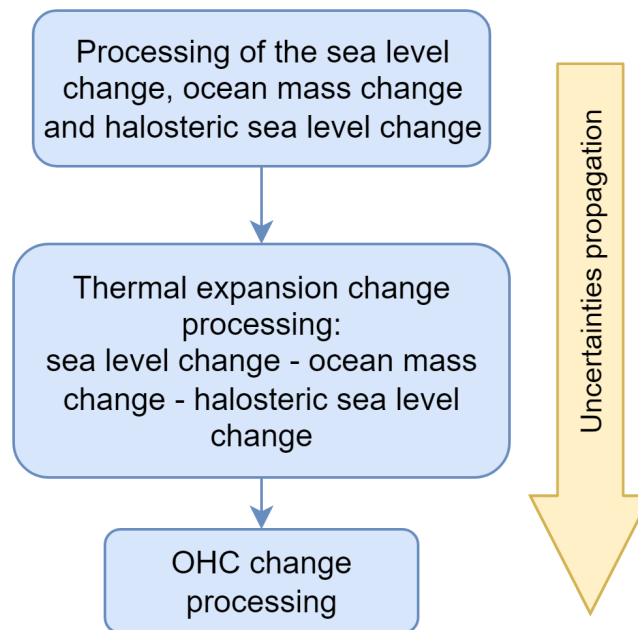
Figure 1: 4DAtlantic processing chain steps for the estimation of OHC change and its uncertainties

This ATBD is divided into 4 sections. We first give a brief summary of the method, then we describe the input data for the processing chain, mainly altimetry, gravimetry and in-situ observations. We then explain how the OHC change is calculated at spatial regional scale before presenting the uncertainty propagation methodology in the last section.

1.3. Document structure

In addition to this introduction, the document is organised as follows:
- Section 2 explains the physical principle of the space geodetic approach and OHC change calculation
- Section 3 provides the description of the input data of the 4DAtlantic processing chain.
- Section 4 provides a detailed description and justification of every step in the OHC computation.
- Section 5 provides a detailed description and justification of the uncertainty propagation methodology until the final OHC product.

1.4. Related documents

1.4.1. Applicable documents

The following table lists the documents with a direct bearing on the content of this document.

This document is property of Magellium. It cannot be reproduced,nor communicated without permission.

page 7/37

Id.	Reference	Name of Document
AD1	OHCATL-DT-035-MAG_Experimental _Dataset_Description	Experimental Dataset Description (EDD) - 4DAtlantic OHC product user manual

Table 1: List of applicable documents

1.4.2. Reference documents

The following table lists the materials which contain information in support of this document.

Id.	Ref.	Description
RD1	-	C3S data store: https://cds.climate.copernicus.eu/
RD2	D3.SL.1-v2.0_PUGS_of_v2DT2 021_SeaLevel_products_v1.1_ APPROVED_Ver1.pdf	Product product user manual of sea level daily gridded data for the global ocean from 1993 to present from Copernicus Climate Change Service (C3S): https://datastore.copernicus-climate.eu/document s/satellite-sea-level/vDT2021/D3.SL.1-v2.0_PUGS _of_v2DT2021_SeaLevel_products_v1.1_APPROVE D_Ver1.pdf
RD3	D1.SL.2-v2.0_ATBD_of_v2DT2 021_SeaLevel_products_v1.1_ APPROVED_Ver1.pdf	Algorithm Theoretical Basis Document of sea level daily gridded data for the global ocean from 1993 to present from Copernicus Climate Change Service (C3S): https://datastore.copernicus-climate.eu/document s/satellite-sea-level/vDT2021/D1.SL.2-v2.0_ATBD _of_v2DT2021_SeaLevel_products_v1.1_APPROVE D_Ver1.pdf
RD4	ftp://ftp.legos.obs-mip.fr/pub/ soa/gravimetrie/grace_legos/V 1.5.1/	Ensemble of the ocean mass solutions provided by Blazquez et al., (2018) on LEGOS FTP site.
RD5	https://grace.jpl.nasa.gov/dat a/data-updates/	Jet Propulsion Laboratory (NASA) website dedicated to Gravity recovery and climate experiment, GRACE and GRACE-FO missions.
RD6	https://www.seanoe.org/data/ 00412/52367/	Sea scientific open data edition (SEANOE) website dedicated to ISAS20 temperature and salinity gridded fields
RD7	https://www.metoffice.gov.uk/ hadobs/en4/download-en4-2-2 .html	Met Office Hadley Center website dedicated to EN4.2.2.l09 temperature and salinity gridded fields
RD8	https://www.ecco-group.org/p roducts-ECCO-V4r4.htm	Ecco groupe website dedicated to ECCO-V4r4 reanalysis product access

Table 2: List of reference documents

magellium

This document is property of Magellium. It cannot be reproduced,nor communicated without permission.

page 8/37

1.5. Terminology

Abbreviation/acronym	Description
AMOC	Atlantic Meridional Overturning Circulation
ATBD	Algorithm theoretical basis document
Argo	International program that uses profiling floats deployed worldwide to observe ocean properties such as temperature and salinity.
C3S	Copernicus Climate Change Service
COST-G	International Combination Service for Time-variable Gravity Fields
EDD	Experimental dataset description
EEH	Expansion efficiency of heat
ESA	European Space Agency
EWH	Equivalent water height
FTP	File transfer protocol
GFZ	Deutsches GeoForschungsZentrum or German research center for geosciences
GIA	Glacial isostatic adjustment
GMWTC	Global mean wet tropospheric correction
GRACE(-FO)	Gravity recovery and climate experiment (-Follow on)
GRD	Changes in Earth Gravity, Earth Rotation and viscoelastic solid-Earth Deformation
GSFC	Goddard Space Flight Center
$(SL_{halosteric})$	Halosteric sea level
IEEH	Integrated expansion efficiency of heat
JPL	Nasa's jet propulsion laboratory
LEGOS	Laboratoire d'Etudes en Géophysique et Océanographie Spatiale
MASL	Manometric Sea Level
MSS	Mean sea surface
MWR	Microwave radiometer
OHC	Ocean heat content
OHU	Ocean heat uptake
OLS	Ordinary least square
RD	Reference document
SL	Absolute Sea level
SLA	Absolute Sea level anomaly

This document is property of Magellium. It cannot be reproduced, nor communicated without permission.

page 9/37

(SL_{steric})	Steric sea level
(SL_{thermo})	Thermosteric sea level

Table 3: List of abbreviations and acronyms

1.6. Bibliography

- Ablain, M., Cazenave, A., Larnicol, G., Balmaseda, M., Cipollini, P., Faugère, Y., Fernandes, M. J., Henry, O., Johannessen, J. A., Knudsen, P., Andersen, O., Legeais, J., Meyssignac, B., Picot, N., Roca, M., Rudenko, S., Scharffenberg, M. G., Stammer, D., Timms, G., and Benveniste, J.: Improved sea level record over the satellite altimetry era (1993–2010) from the Climate Change Initiative project, Ocean Sci., 11, 67–82, https://doi.org/10.5194/os-11-67-2015, 2015.
- Ablain, M., Meyssignac, B., Zawadzki, L., Jugier, R., Ribes, A., Spada, G., Benveniste, J., Cazenave, A., and Picot, N.: Uncertainty in satellite estimates of global mean sea-level changes, trend and acceleration, Earth Syst. Sci. Data, 11, 1189–1202, https://doi.org/10.5194/essd-11-1189-2019, 2019.
- Barnoud, A., Pfeffer, J., Guérou, A., Frery, M., Siméon, M., Cazenave, A., Chen, J., Llovel, W., Thierry, V., Legeais, J., and Ablain, M.: Contributions of Altimetry and Argo to Non-Closure of the Global Mean Sea Level Budget Since 2016, Geophys. Res. Lett., 48, e2021GL092824, https://doi.org/10.1029/2021GL092824, 2021.
- Barnoud, A., Picard, B., Meyssignac, B., Marti, F., Ablain, M., and Roca, R.: Reducing the long term uncertainties of global mean sea level using highly stable water vapour climate data records, in revision.
- Barnoud, A., Pfeffer, J., Cazenave, A., and Ablain, M.: Revisiting the global ocean mass budget over 2005-2020, in prep.
- Blazquez, A., Meyssignac, B., Lemoine, J., Berthier, E., Ribes, A., and Cazenave, A.: Exploring the uncertainty in GRACE estimates of the mass redistributions at the Earth surface: implications for the global water and sea level budgets, Geophys. J. Int., 215, 415–430, https://doi.org/10.1093/gji/ggy293, 2018.
- Caron, L., Ivins, E. R., Larour, E., Adhikari, S., Nilsson, J., and Blewitt, G.: GIA Model Statistics for GRACE Hydrology, Cryosphere, and Ocean Science, Geophys. Res. Lett., 45, 2203–2212, https://doi.org/10.1002/2017GL076644, 2018.
- Carrère, L. and Lyard, F.: Modeling the barotropic response of the global ocean to atmospheric wind and pressure forcing - comparisons with observations, Geophys. Res. Lett., 30, 1275, https://doi.org/10.1029/2002GL016473, 2003.
- Cheng, L., Trenberth, K. E., Fasullo, J., Boyer, T., Abraham, J., and Zhu, J.: Improved estimates of ocean heat content from 1960 to 2015, Sci. Adv., 3, e1601545, 2017.
- Cheng, M., Tapley, B. D., and Ries, J. C.: Deceleration in the Earth's oblateness, J. Geophys. Res. Solid Earth, 118, 740–747, https://doi.org/10.1002/jgrb.50058, 2013.
- Dahle, C., Flechtner, F., Murböck, M., Michalak, G., Neumayer, H., Abrykosov, O., Reinhold, A., and König, R.: GRACE Geopotential GSM Coefficients GFZ RL06 (6.0), https://doi.org/10.5880/GFZ.GRACE_06_GSM, 2018.
- ECCO Consortium, Fukumori, I., Wang, O., Fenty, I., Forget, G., Heimbach, P., and Ponte, R. M.: Synopsis of the ECCO central production global ocean and sea-ice state estimate (version 4 release 4), Zenodo, 2020.
- Forget, G., Campin, J.-M., Heimbach, P., Hill, C., Ponte, R., and Wunsch, C.: ECCO version 4: An integrated framework for non-linear inverse modeling and global ocean

This document is property of Magellium. It cannot be reproduced, nor communicated without permission.

page 10/37

state estimation, Geosci. Model Dev., 8, 3071–3104, 2015.

- Frederikse, T., Riva, R. E. M., and King, M. A.: Ocean Bottom Deformation Due To Present-Day Mass Redistribution and Its Impact on Sea Level Observations, Geophys. Res. Lett., 44, 12,306-12,314, https://doi.org/10.1002/2017GL075419, 2017.

- Gaillard, F., Reynaud, T., Thierry, V., Kolodziejczyk, N., and Schuckmann, K. von: In Situ–Based Reanalysis of the Global Ocean Temperature and Salinity with ISAS: Variability of the Heat Content and Steric Height, J. Clim., 29, 1305–1323, https://doi.org/10.1175/JCLI-D-15-0028.1, 2016.

- Good, S. A., Martin, M. J., and Rayner, N. A.: EN4: Quality controlled ocean temperature and salinity profiles and monthly objective analyses with uncertainty estimates, J. Geophys. Res. Oceans, 118, 6704–6716, https://doi.org/10.1002/2013JC009067, 2013.

- Hosoda, S., Ohira, T., Sato, K., and Suga, T.: Improved description of global mixed-layer depth using Argo profiling floats, J. Oceanogr., 66, 773–787, https://doi.org/10.1007/s10872-010-0063-3, 2010.

- Kuhlbrodt, T. and Gregory, J. M.: Ocean heat uptake and its consequences for the magnitude of sea level rise and climate change, Geophys. Res. Lett., 39, https://doi.org/10.1029/2012GL052952, 2012.

- Legeais, J.-F., Meyssignac, B., Faugère, Y., Guerou, A., Ablain, M., Pujol, M.-I., Dufau, C., and Dibarboure, G.: Copernicus Sea Level Space Observations: A Basis for Assessing Mitigation and Developing Adaptation Strategies to Sea Level Rise, Front. Mar. Sci., 8, 2021.

- Lemoine, J. and Reinquin, F.: Processing of SLR observations at CNES, Newsl. EGSIEM, 3, 2017.

- Lemoine, J.-M. and Bourgogne, S.: RL05 monthly and 10-day gravity field solutions from CNES/GRGS, Copernicus Meetings, https://doi.org/10.5194/gstm2020-51, 2020.

- Levitus, S., Antonov, J. I., Boyer, T. P., Locarnini, R. A., Garcia, H. E., and Mishonov, A. V.: Global ocean heat content 1955-2008 in light of recently revealed instrumentation problems: GLOBAL OCEAN HEAT CONTENT, Geophys. Res. Lett., 36, n/a-n/a, https://doi.org/10.1029/2008GL037155, 2009.

- Levitus, S., Antonov, J. I., Boyer, T. P., Baranova, O. K., Garcia, H. E., Locarnini, R. A., Mishonov, A. V., Reagan, J. R., Seidov, D., Yarosh, E. S., and Zweng, M. M.: World ocean heat content and thermosteric sea level change (0–2000 m), 1955–2010, Geophys. Res. Lett., 39, https://doi.org/10.1029/2012GL051106, 2012.

- Loomis, B. D., Rachlin, K. E., and Luthcke, S. B.: Improved Earth Oblateness Rate Reveals Increased Ice Sheet Losses and Mass-Driven Sea Level Rise, Geophys. Res. Lett., 46, 6910–6917, https://doi.org/10.1029/2019GL082929, 2019.

- Marti, F., Blazquez, A., Meyssignac, B., Ablain, M., Barnoud, A., Fraudeau, R., Jugier, R., Chenal, J., Larnicol, G., Pfeffer, J., Restano, M., and Benveniste, J.: Monitoring the ocean heat content change and the Earth energy imbalance from space altimetry and space gravimetry, Earth Syst. Sci. Data, 14, 229–249, https://doi.org/10.5194/essd-14-229-2022, 2022a.

- Marti, F., Blazquez, A., Meyssignac, B., Ablain, M., Barnoud, A., Fraudeau, R., Jugier, R., Chenal, J., Larnicol, G., Pfeffer, J., Restano, M., and Benveniste, J.: Monitoring the ocean heat content change and the Earth energy imbalance from space altimetry and space gravimetry, Earth Syst. Sci. Data, https://doi.org/10.5194/essd-2021-220, 2022b.

- Mayer-Gürr, T., Behzadpur, S., Ellmer, M., Kvas, A., Klinger, B., Strasser, S., and Zehentner, N.: ITSG-Grace2018 - Monthly, Daily and Static Gravity Field Solutions from GRACE, https://doi.org/10.5880/ICGEM.2018.003, 2018.

- Meyssignac, B., Boyer, T., Zhao, Z., Hakuba, M. Z., Landerer, F. W., Stammer, D., Köhl, A., Kato, S., L'Ecuyer, T., Ablain, M., Abraham, J. P., Blazquez, A., Cazenave, A., Church,

This document is property of Magellium. It cannot be reproduced, nor communicated without permission.

page 11/37

J. A., Cowley, R., Cheng, L., Domingues, C. M., Giglio, D., Gouretski, V., Ishii, M., Johnson, G. C., Killick, R. E., Legler, D., Llovel, W., Lyman, J., Palmer, M. D., Piotrowicz, S., Purkey, S. G., Roemmich, D., Roca, R., Savita, A., Schuckmann, K. von, Speich, S., Stephens, G., Wang, G., Wijffels, S. E., and Zilberman, N.: Measuring Global Ocean Heat Content to Estimate the Earth Energy Imbalance, Front. Mar. Sci., 6, https://doi.org/10.3389/fmars.2019.00432, 2019.

- Peltier, W. R., Argus, D. F., and Drummond, R.: Comment on "An Assessment of the ICE-6G_C (VM5a) Glacial Isostatic Adjustment Model" by Purcell et al., J. Geophys. Res. Solid Earth, 123, 2019–2028, https://doi.org/10.1002/2016JB013844, 2018.
- Prandi, P., Meyssignac, B., Ablain, M., Spada, G., Ribes, A., and Benveniste, J.: Local sea level trends, accelerations and uncertainties over 1993–2019, Sci. Data, 8, 1, https://doi.org/10.1038/s41597-020-00786-7, 2021.
- Roemmich, D., Johnson, G. C., Riser, S., Davis, R., Gilson, J., OWENS, W. B., GARZOLI, S. L., SCHMID, C., and IGNASZEWSKI, M.: The Argo Program, Oceanography, 22, 34–43, 2009.
- Russell, G. L., Gornitz, V., and Miller, J. R.: Regional sea level changes projected by the NASA/GISS Atmosphere-Ocean Model, Clim. Dyn., 16, 789–797, https://doi.org/10.1007/s003820000090, 2000.
- Spada, G. and Melini, D.: On Some Properties of the Glacial Isostatic Adjustment Fingerprints, Water, 11, 1844, https://doi.org/10.3390/w11091844, 2019.
- Sun, Y., Riva, R., and Ditmar, P.: Optimizing estimates of annual variations and trends in geocenter motion and J2 from a combination of GRACE data and geophysical models, J. Geophys. Res. Solid Earth, 121, 8352–8370, https://doi.org/10.1002/2016JB013073, 2016.
- Taylor, J. R.: An Introduction to Error Analysis: The Study of Uncertainties in Physical Measurements, 2nd ed., University Science Books, Sausalito, California, 344 pp., 1997.
- WCRP Global Sea Level Budget Group: Global sea-level budget 1993–present, Earth Syst. Sci. Data, 10, 1551–1590, https://doi.org/10.5194/essd-10-1551-2018, 2018.
- Yuan, D.: GRACE Follow-On level-2 gravity field product user handbook, Jet Propuls. Lab. JPL -103922, 2019.

2. Physical principle

In this document, the word "change" refers to the difference between any two states - it refers to the difference between the present state (t) and the state to a given date (t_{ref}) or time period.

This regional OHC change is derived from the **Steric Sea Level (SSL) change**. For this purpose, a coefficient of expansion efficiency of heat is needed to do the conversion of thermal expansion into OHC change.

2.1. The (Integrated) Expansion Efficiency of Heat

The expansion efficiency of heat (EEH) expresses the change in ocean density due to heat uptake. As a matter of fact it represents the ratio of the temporal derivative of thermosteric sea level over the temporal derivative of the heat content under a given heat uptake. The EEH

magellium

This document is property of Magellium. It cannot be reproduced,nor communicated without permission.

page 12/37

is dependent on temperature, salinity and pressure (Russell et al., 2000). Thus, integrated over the total water column, the EEH is supposed to vary with latitude along with the variations of integrated salinity, temperature and pressure. At a regional scale, the EEH has never been calculated. To explain this, it occurs that the OHC change over an entire water column can be null whilst the thermal expansion is not. In such a situation, the EEH is not defined and cannot be calculated. A way to avoid this issue is to consider the **integrated expansion efficiency of heat (IEEH)** instead of the EEH (Marti et al., 2022a).. The IEEH must reflect the variation in sea level due to a change in its heat content. The idea is to use in-situ products to calculate the IEEH (see section 3), which is assumed to be a characteristic of the water column, allowing a variation in steric level to be converted into a variation in OHC thanks to this proportionality coefficient. It is important to note that the IEEH is independent of the measurement system used.

$$IEEH = \frac{\delta SL_{thermo}}{\delta OHC}$$

Eq. 1

2.2. OHC calculation

The OHC estimated from satellite measurement of steric sea level can therefore be deduced from the in-situ OHC by doing the following. :

$$(\Delta OHC)_{sat} = (\Delta OHC)_{in\ situ} + \frac{(\Delta SL_{thermo})_{sat} - (\Delta SL_{thermo})_{in\ situ}}{(IEEH)_{in\ situ}}$$

Eq. 2

The absolute height of the thermosteric sea level is not accessible by satellite; only its steric variations are available.

We need to define a reference date where we assume that $(\Delta OHC)_{sat} = (\Delta OHC)_{in\ situ}$ and $(\Delta SL_{steric})_{sat} = (\Delta SL_{steric})_{in\ situ} = (\Delta SL_{steric})_{ref}$

$$(\Delta OHC)_{sat} - (\Delta OHC)_{in\ situ} =$$

Eq. 3

$$\frac{((\Delta SL_{thermo})_{sat} + (\Delta SL_{halo}) - (\Delta SL_{steric})_{ref}) - ((\Delta SL_{thermo})_{in\ situ} + (\Delta SL_{halo}) - (\Delta SL_{steric})_{ref})}{IEEH_{insitu}} =$$

$$\frac{(\Delta SL_{steric})_{sat} - (\Delta SL_{steric})_{in\ situ}}{(IEEH)_{in\ situ}}$$

magellium

This document is property of Magellium. It cannot be reproduced, nor communicated without permission.

page 13/37

Satellite OHC can be calculated from in-situ OHC, IEEH, and satellite and in-situ steric sea level change. The estimation of the various components of this formula is explained in section 3.

2.2.1. Constancy of the IEEH

The IEEH shows regional variations due to ocean temperature and volume changes which may be induced by factors such as ocean currents and atmospheric circulation patterns. However, at the global scale the IEEH can be considered as constant (Eq. 4), with typical trends being less than 0.03% per decade. This means that at the global scale, the ocean is considered a large and well mixed body of water.

$$(IEEH)_{in\ situ}(t) = (IEEH)_{in\ situ}(t_0)$$

Eq. 4

3. Input data

3.1. Overview

The following section describes the different datasets used for the computation of the OHC change grids. They include time-varying data such as the total Absolute Sea Level (ΔSL) change, the Manometric Sea Level (ΔMASL) change and the integrated expansion efficiency of heat, which is used to convert thermal expansion change into ocean heat content change. There is also static data such as the water ratio, grid cells area and the Glacial Isostatic Adjustment. These inputs are spatial data given on the entire globe. However, their spatial availability is different and may vary over time. The origin and format of each dataset are described in a dedicated subsection. The limitations and errors associated with the dynamic input datasets are also presented.

3.2. Manometric sea level

Manometric sea level (MASL) change estimates are derived from gravimetric measurements from 04/2002 to 07/2022.

3.2.0.1. Description of gravimetry data

GRACE and GRACE Follow On (GRACE-FO) missions provide the Earth's surface mass changes. As GRACE data are impacted by different error sources (Blazquez et al., 2018; Meyssignac et

This document is property of Magellium. It cannot be reproduced,nor communicated without permission.

page 14/37

al., 2019), we used an ensemble approach in order to average the errors and also to evaluate the uncertainty in manometric sea level.

Blazquez et al. (2018) provided an ensemble of ΔMASL solutions derived from GRACE with a range of state-of-the-art post-processing parameters to get a spread of GRACE estimates of the manometric sea level.

For this study we used an update of the ensemble from Blazquez et al. (2018). The version v2.0 that is used is estimated with a new processing chain. The main advantage of this ensemble processing chain is that it is capable of handling different spherical harmonic solutions (L2) as input, as well as different post-processing solutions, to ultimately generate a set of gravimetric solutions (L3).

The set is based on the Earth's gravitational potential field estimated by five different centers, expressed in Stokes coefficients (i.e. in the spherical harmonic basis) up to degree 96, including JPL (RL06, NASA Jet Propulsion Laboratory (JPL), 2019; Yuan, 2019), CSR (RL06; Yuan, 2019), GFZ (RL06, Dahle et al., 2018), ITSG (GRACE2018, Mayer-Gürr et al., 2018) and CNES-GRGS (RL05, Lemoine and Bourgogne, 2020). However, these coefficients are affected by several sources of error and limitations that need to be corrected in several post-processing steps. For these 5 centers, 24 post-processings are available, leading to a combination of 120 solutions.

The list of the various post-processings is as follows:

- 1 geocenter model (degree 1 coefficients) provided by (Lemoine and Reinquin, 2017; Sun et al., 2016). This correction is necessary because the GRACE and GRACE-FO satellites orbit around the center of mass and are therefore not sensitive to geocenter motion. They cannot be used to evaluate Stokes coefficients of degree 1.
- 3 SLR (Satellite Laser Ranging) products to estimate low-degree coefficients (C20 and C30) provided by Cheng et al., (2013); Lemoine and Reinquin, (2017); Loomis et al., (2019). These data are more robust, as GRACE and GRACE-FO measurements are not very sensitive to low degrees.
- 2 GIA models provided by (Caron et al., 2018; Peltier et al., 2018) are used to correct for deglaciation-induced viscoelastic Earth deformations.
- 2 types of DDK filters to correct systematic correlated errors (easily identifiable north-south striations).

Additional corrections are applied identically to all ensemble members, linked to dealiasing patterns and leakage errors. This set of solutions is then used to estimate the uncertainty in the gravity data associated with the processing and post-processing of the measurements, by calculating the standard deviation of the ensemble. This led to a new ensemble of 60 solutions.

ΔMASL data is described and available in NetCDF format file on the following LEGOS FTP [Table 2, RD4]. Its content is described below:

- Ensemble of 60 ΔMASL solutions and its ensemble mean
  - units: m water height thickness (WHT)
  - spatial resolution: 1° x 1°
  - temporal resolution: monthly
  - temporal availability: April 2002 - September 2023
  - version: v2.0

3.2.1. Comments/limitations

As explained in Blazquez et al. (2018), the combination of the different raw solutions (from processing centers) with the different post-processing parameters (geocenter motion

correction, filtering techniques, leakage and GIA corrections) leads to an ensemble which is assumed to cover a significant part of the uncertainty range of GRACE/GRACE-FO manometric sea level estimates.

For this reason, the entire 60 solutions ensemble is used to estimate the MASL change uncertainties at regional scale (see section 5.4.2.).

Uncertainties on the estimation of the geocenter correction is for now taken into account since only one solution is provided in the ensemble (Lemoine and Reinquin, 2017; Sun et al., 2016). Uncertainty regarding this correction which has an important impact on the ocean mass estimates will be evaluated in the future versions of the product.

3.3. Absolute Sea level

3.3.1. Description

Absolute Sea Level (SL) change at regional scales are derived from the sea-level products operationally generated by the Copernicus Climate Change Service (C3S). This dataset, fully described in (Legeais et al., 2021) is dedicated to the sea level stability for climate applications. It provides daily sea-level anomalies grids based at any time on a reference altimeter mission (TopEx/Poseidon, Jason-1,2,3 and S6-MF) plus complementary missions (ERS-1,2, Envisat, Cryosat, SARAL/Altika, Sentinel-3A) to increase spatial coverage.

C3S provides the absolute sea level anomaly (SLA) around a mean sea surface (MSS) above the reference mean sea-surface computed over 1993-2012, or in other words, the total SL change [Table 2, RD2]. Data is available in NetCDF format files on the C3S data store [Table 2, RD1]. The main characteristics of SLA grids are:

- spatial resolution: 0.25° x 0.25°
- temporal resolution: daily
- temporal availability: altimetry era, January 1993 - May 2023
- units: m
- version: vDT2021

More information is available in the product user manual of C3S [RD2] and the algorithm description document [RD3].

3.3.2. Comments/limitations

C3S data result from the most up-to-date standards (altimeter standards, geophysical corrections) whose timeliness is compatible with the C3S production planning and most of them follow the recommendations of the ESA Sea Level CCI project. They are submitted to a rigorous validation process.

However, these data are affected by errors like any spatial measurements. The full description of these errors was already described at global scale (Ablain et al., 2015, 2019). In a further study, a full estimation of the regional altimetry error budget was used to derive regional error variance-covariance matrices (Prandi et al., 2021). These error matrices are well adapted to

This document is property of Magellium. It cannot be reproduced,nor communicated without permission.

page 16/37

the description of C3S data measurements because the SL errors are the same (similar altimeter standards). It has therefore been used as an input for the error propagation purpose in this project (see section 5. devoted to this topic).

3.3.3. Specific corrections

Grids of absolute sea level change provided by C3S do not take in consideration the global isostatic adjustment (GIA) process in response to the melting of the Late Pleistocene ice sheets. However, this effect needs to be corrected in absolute sea level change estimates as it does not reflect the ocean's response to recent climate change. GIA contains regional variations that must be corrected. It is still an area of active research, and then several GIA grids expressed as trends in lithospheric height change (in mm/year) are available in the litterature. The same GIA correction used in the recent study (Prandi et al., 2021) for an estimation of the absolute sea level trends uncertainties at regional scale has been applied. It is an ensemble mean of the regional GIA results for model ICE-5G, with various viscosity profiles (27 profiles). The methodology is also described in (Spada and Melini, 2019). The average GIA value over oceans from this 27 solution ensemble is 0,33 mm.yr^{-1} closely matching the value of -0.3 mm.yr^{-1} (WCRP Global Sea Level Budget Group, 2018), generally adopted as a rule of thumb to correct the altimetric absolute sea-level trend for the effects of past GIA.

An additional correction is considered to take into account the ocean bottom deformation due to present-day mass redistribution. This correction GRD (changes in Earth Gravity, Earth Rotation and viscoelastic solid-Earth Deformation) has been evaluated at 0.1 mm/yr during the altimetry area (1993-2014), (Frederikse et al., 2017). We have applied this correction only on absolute sea level observations because this effect has no impact on the gravimetric data. The constant value is used in the regional computation.

magellium

This document is property of Magellium. It cannot be reproduced,nor communicated without permission.

page 17/37
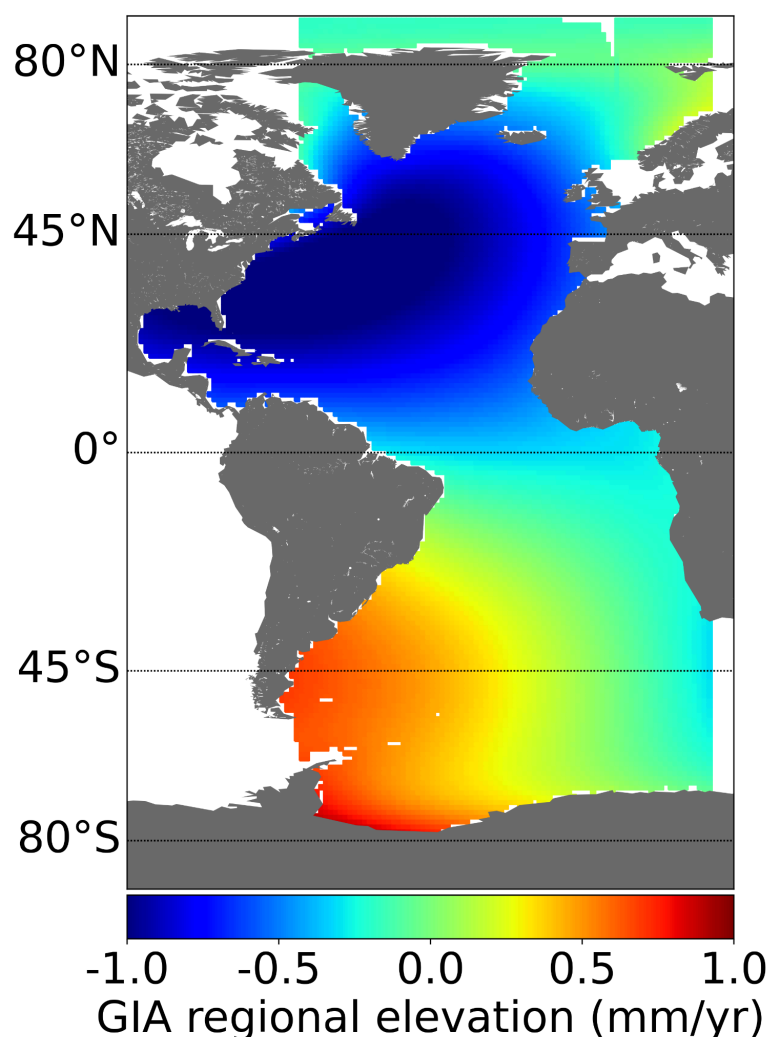
Figure 2: Regional grid of the GIA correction applied to altimetry absolute sea level grids in 4DAtlantic processing chain (Spada and Melini, 2019)

Moreover, recent studies have shown that a drift on Jason-3 radiometer has been detected and a correction should be applied on sea level grids. This correction was calculated from the relative differences between the global mean wet tropospheric correction (GMWTC) from Jason-3 microwave radiometer (MWR) and the GMWTC derived from water vapour climate data records (Barnoud et al., in revision), the GMWTC from SARAL/AltiKa's MWR and the GMWTC from Sentinel-3A. The correction C_{J3} is computed as the average of the zero-mean GMWTC differences (Barnoud et al., in prep.).

This document is property of Magellium. It cannot be reproduced, nor communicated without permission.

page 18/37

3.4. In situ data

3.4.1. Steric sea level

3.4.1.1. Description
Steric sea level represents the difference in water height between a given column and the same column whose conservative temperature and absolute salinity would be equal to a fixed reference.

3.4.1.2. Regional estimates of the steric sea level
The steric sea level SSL(t,lat,lon) of the whole water column is referenced to a physical thermosteric sea-level content (defined at 0° Celsius and 35 PSU) and calculated from in-situ measurements of temperature and salinity following:

$$(SL_{steric})_{in\ situ} = [\Sigma_j \ \frac{(\rho_{ref} - \rho(T,S,\Sigma_i h_i)).|h_j|}{\rho_{ref}}]_{t,lat,lon}$$

Eq. 5

Finally, the main characteristics of $(SL_{steric})_{in\ situ}$ grids are:

- spatial resolution: 1° x 1°
- temporal resolution: monthly
- depth integration: EN4.2.2.l09 data [RD7] for the 0-6000m depth (Levitus et al., 2009).
- temporal average: January 1993 - May 2023
- units: m

Since salinity drift is present in the EN4 dataset (Barnoud et al., 2021), the salinity of the product has been replaced to its climatology estimated over the period 2005-2015 before computing the $(SL_{steric})_{in\ situ}$.

3.4.2. Regional estimates of the OHC

The ocean heat content OHC(t,lat,lon) of the whole water column is calculated from in-situ measurements of temperature and salinity following:

$$(OHC)_{insitu} = [\Sigma_j \ \rho. C_p. C_t]_{t,lat,lon}$$

Eq. 6

With ρ the density $kg.m^3$, C_p the heat capacity in $J.kg^{-1}.°C$ and C_t the conservative temperature in °C.
Finally, the main characteristics of OHC grids are:
- spatial resolution: 1° x 1°

This document is property of Magellium. It cannot be reproduced,nor communicated without permission.

page 19/37

- temporal resolution: monthly
- depth integration: EN4.2.2.l09 data [RD7] for the 0-6000m depth (Levitus et al., 2009).
- temporal average: January 1993 - May 2023
- units: J

Since salinity drift is present in the EN4.2.2.l09 dataset (Barnoud et al., 2021), the salinity of the product has been replaced to its climatology estimated over the period 2005-2015 before computing the $(OHC)_{in\ situ}$.

3.4.3. Integrated Expansion Efficiency of Heat

3.4.3.1. Description

The integrated expansion efficiency of heat (IEEH) reflects the variation in sea level due to a change in its heat content.

3.4.3.2. Regional estimates of the integrated EEH

In the framework of this project, IEEH values are provided as 3D grids defined at regional scales with a 1-degree spatial resolution and at monthly timescale. They are calculated based on in situ temperature and salinity fields. IEEH is defined as the ratio between SSL change and OHC change:

$$(IEEH)_{in\ situ} = surf_{cell} * \frac{(SL_{steric})_{in\ situ}(T,S) - (SL_{steric})_{in\ situ}(T_{clim},S)}{(OHC)_{in\ situ}(T,S) - (OHC)_{in\ situ}(T_{clim},S)} \qquad \text{Eq. 6}$$

where :
- $surf_{cell}$ the ocean cell surface
- SSL is the steric sea-level of the whole water column as estimated above in Eq. 5
- OHC(t,lat,lon) is the ocean heat content integrated over the whole water column and is calculated following:

$$(OHC)_{in\ situ} = [\Sigma_j \ \rho(T,S,\Sigma_i h_i).\ C_p(T,S,\Sigma_i h_i).\ CT(T,S,\Sigma_i h_i).\ |h_j|] \qquad \text{Eq. 7}$$

Where
- h_j is the j-th value of the thickness layer so that $\Sigma_i h_i$ is the depth of integration (in m),
- ρ_{ref} is the reference value of the density computed at fixed Salinity (35psu) and Temperature (0°C),
- $\rho(T,S,\Sigma_i h_i)$ is the density calculated based on salinity and temperature variations,
- $\rho(T,S_{clim},\Sigma_i h_i)$ is the density with salinity fixed at the climatology,
- $CT(T,S,\Sigma_i h_i)$ is the conservative temperature (in $°C$) and,

magellium

This document is property of Magellium. It cannot be reproduced,nor communicated without permission.

page 20/37

.

- $C_p(T, S, \Sigma_i h_i)$ is the heat capacity of sea water (in $J.kg^{-1}.{}^\circ C^{-1}$)

Note that SSL and OHC changes are locally filtered with a cutoff period of 3 years before estimating the IEEH. This high-frequency variability can arise from various sources, such as local weather conditions, ocean currents, and internal ocean waves. These high-frequency signals can mask the underlying signal of interest, which is the long-term trend in ocean thermal expansion. In this way, the IEEH coefficient gives the OHC for the whole water column for a variation of thermosteric sea level around a physical reference. ECCO dataset [RD8] is used to compute the (SL_{thermo}) change and OHC change over 0-6000 m depth. Afterwards we can take the time-mean of the time varying IEEH over a chosen period to estimate the time-mean IEEH which is used to estimate the OHC change (Figure 3).
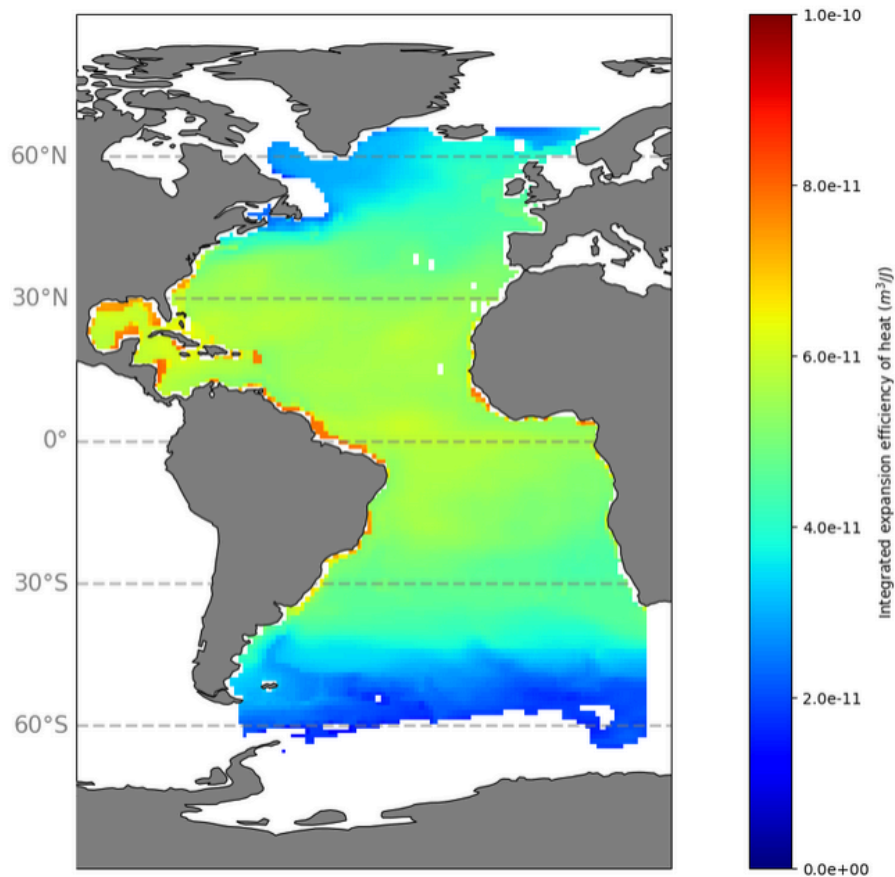
Figure 3: Time-mean of the Integrated Expansion Efficiency of Heat (IEEH) coefficients (m³/J) (1x1 degree).

Finally, the main characteristics of IEEH grids are:
- spatial resolution: 1° x 1°
- temporal resolution: monthly
- depth integration: ECCO-V4r4 data [RD6] for the 0-6000m depth (ECCO Consortium et al., 2020; Forget et al., 2015).

magellium

This document is property of Magellium. It cannot be reproduced,nor communicated without permission.

page 21/37

- temporal average: mean of January 2005 - December 2015
- units: m³/J

3.4.3.3. Comments/limitations

To assess the uncertainties on the OHC derived from data at local scale, the uncertainty on the IEEH is required. To estimate this value, the dispersion of several in situ products have been used (more details in the "Uncertainty" section.

3.5. Static data: water ratio

When manipulating data at regional scales, it is necessary to know the proportion of ocean in each cell for grid's downsampling or deriving the global mean for instance.

A water ratio grid is computed from distance to coast information and provides the part of water surface in each cell of the grid between 0 and 1. Distance to coast data is provided by the NASA Goddard Space Flight Center (GSFC) Ocean Color Group and given on a 0.01° resolution grid.

3.6. Static data: grid cells area

When manipulating data at regional scales, it is necessary to know the area of each cell for grid's downsampling or deriving the global mean for instance. The surface is computed for each grid cell taking the Earth oblateness into consideration.

4. 4DAtlantic OHC processing chain

4.1. Outline

The regional approach allows us to know the spatial distribution of ocean heat content change, which is essential for understanding the role of the Atlantic Ocean in the climate system.

As the OHC change is computed from the combination of altimetry-gravimetry spatial observations and the removal of the halosteric component calculated with in-situ Argo floats, its spatial and temporal characteristics depend on these measurements. OHC change characteristics will be constrained by the limitations of gravimetry observations and in-situ data both at spatial and temporal scales. Effective temporal and spatial resolutions of GRACE(-FO) products is 1 month and 300 km and it is of 1 month and 100 km for in-situ Argo products. However it is about 10-days at about 100 km for level-4 altimetry products. Therefore the regional OHC change grids in the 4DAtlantic project have been defined at 1°x1° resolution and on a monthly basis. As a reminder, the variables noted SL and MASL change are not absolute quantities but anomalies with respect to a reference (see sections 3.2.1., 3.3.1., 3.4.1.). In the following, we will define the reference of (SL_{steric}) and OHC change.

This document is property of Magellium. It cannot be reproduced,nor communicated without permission.

page 22/37

The Figure 4 below describes the 4DAtlantic processing chain with its main algorithms for generating OHC data from input altimetry-gravimetry and in-situ data. The following subsections describe the algorithms developed in detail.
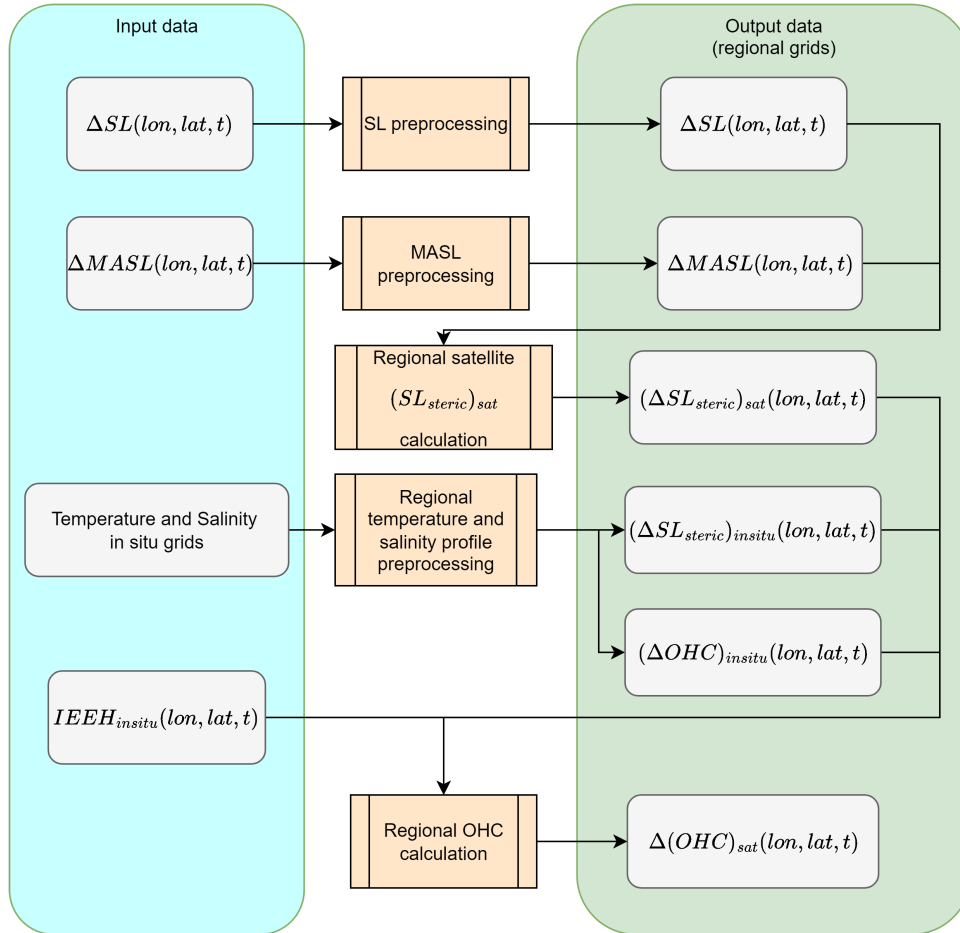
Figure 4: Overview of the 4DAtlantic processing chain. Variables are given with their dimensions (lon: longitude, lat: latitude, t: time)

4.2. Input data

The 4DAtlantic processing chain, which allows to compute the OHC change variable, is configured to use the following input data, described in section 3..

- MASL change gridded data (spatial resolution: 1°x 1° - temporal resolution: monthly)
- SL change gridded data (spatial resolution: 0.25°x 0.25° - temporal resolution: daily)
- (SL_{steric}) and OHC change gridded data from in-situ (spatial resolution: 1°x 1° - temporal resolution: monthly)
- IEEH gridded data (spatial resolution: 1°x 1° - temporal resolution: monthly)

This document is property of Magellium. It cannot be reproduced, nor communicated without permission.

page 23/37

- land mask (spatial resolution: 1° x 1°)

4.3. Output data

The 4DAtlantic main product contains the OHC change produced by the processing chain and described in Figure 4 for each month from April 2002 to December 2022:
- OHC change grids
- Variances-covariance matrices for OHC change at every location
- OHC change quality flag (which indicates the data that are interpolated, due to gap of gravimetric data between GRACE and GRACE-FO)

The format of the 4DAtlantic product is described in detail in the 4DAtlantic Experimental Dataset Description (EDD) [Table 1, AD1].

An additional product is available upon request which contain other variables, mainly the intermediate variables (cf EDD) [Table 1, AD1].

4.4. Retrieval methodology

4.4.1. Overview

The algorithms applied in the 4DAtlantic processing chain are described in the following subsections in agreement with Figure 4:
- the preprocessing of regional SL change grids
- the preprocessing of regional MASL change grids
- the calculation of regional (SL_{steric}) change grids
- the calculation of regional OHC change grids

For each algorithm, the objectives, the main mathematical statements and the limitations and any comments about the approach are presented.

4.4.2. Preprocessing of SL change grids

4.4.2.1. Description

The objective of the preprocessing of the SL change grids is to modify the temporal and spatial resolutions of SL change grids used as input data. Indeed, altimetry data used in the 4DAtlantic processing chain is provided by C3S and are given on a daily basis at 0.25x0.25 degrees resolution. Altimetry data need to be downsampled to 1x1 degrees resolution and at the monthly time step to be compared to MASL change grids.

Moreover, the sea level regional grids from C3S are not corrected from the glacial isostatic adjustment (GIA), the elastic effect of the contemporary land ice melting (GRD) and Jason-3 drift. To estimate OHC change, specific corrections must be applied.

This document is property of Magellium. It cannot be reproduced,nor communicated without permission.

page 24/37

4.4.2.2. Mathematical statement

4.4.2.2.1. Temporal interpolation

In order to calculate the SL change grids on a monthly basis (i.e. to switch from a daily to a monthly temporal resolution), a basic average of the N grids of the month is performed. Cells with default values are not taken into account. The monthly averages are kept for each cell regardless of the number of valid values over the month.

4.4.2.2.2. Spatial filtering

The monthly grids are first spatially filtered with a lanczos filter along the longitude and latitude coordinates. The cut-off length is chosen at 150kms and allows to filter out high frequency spatial scales in the sea level which are not present in the gravimetry and halosteric datasets.

4.4.2.2.3. Spatial interpolation

The monthly grids are then computed at a higher spatial resolution: 1x1 degrees instead of 0.25x0.25 degrees. The method applied consists in applying an average of the 4 cells located at the center of a box composed of 16 cells after the application of the Lanczos filter on the grids. This average will be the new value of the full 16 cells box which is 1° sided.

4.4.2.2.4. Corrections applied

Several corrections are applied to the absolute sea level change grids (see section 3.3.3.). The GIA unstructured ensemble mean grid is first sampled on a regular 1 degree resolution grid using linear interpolation. Regional absolute sea level change grids are finally corrected from the GIA correction, the GRD correction and the Jason-3 drift :

$$\Delta SL(x, y, t) \ - \ GIA(x, y) \ - \ GRD(x, y) \ - \ C_{J3}(t) \qquad\qquad \text{Eq. 7}$$

4.4.2.3. Comments/limitations

With regards to the GIA correction, it is still an area of active research. However the impact at regional scales is mainly significant at high latitudes (e.g. discrepancies can reach 0.5-1 mm/yr) where, for the moment, limited information is provided in the 4DAtlantic product due the application of a restrictive geographical mask based on Argo data (see below for more details).

With regards to the Jason-3 drift correction, it was derived to correct the global mean SL. Here an approximation is made by applying this correction at regional scales.

4.4.3. Preprocessing of MASL change grids

4.4.3.1. Description

Gravimetry data used in the 4DAtlantic processing chain are provided at 1°x 1° resolution and monthly time step. MASL change grids are already at a good spatial and temporal resolution.

magellium
artal group

This document is property of Magellium. It cannot be reproduced,nor communicated without permission.

page 25/37

Hence, the objective of the preprocessing of the MASL change grids is to fill the data gaps of the GRACE(-FO) in the ocean mass change grids.

4.4.3.2. Mathematical statement

4.4.3.2.1. Management of the data gap

The MASL change grids contain several gaps due to degradation of the operational capability of GRACE and GRACE-FO and the transition time between the two missions. An implementation of a gap filling algorithm has been made in the product chain generation. This algorithm is described as follows:

- Calculation of the climatological signal: removal of the trend and calculation of the average for each month of the year
- Removal of the climatological signal over the whole time series
- Cubic approximation of the time series to fill in the gaps
- Adding the climate signal to the whole time series (including the gap)

This gap filling algorithm has been applied at regional scales, i.e for each element of the MASL change grids.

An important feature brought by the gap algorithm to the OHC change product is a quality flag which distinguishes between months for which there is data from observations and those for which there is data from interpolation of MASL change. A more detailed explanation of this quality flag is given in the EDD [Table 1, AD1].

4.4.3.2.2. Addition of a high frequency component into the data gaps

The gap-filling algorithm underestimates the part of the signal driven by sub-annual processes. By construction, the high frequency content of the Barystatic Sea Level (BASL) uncertainty estimates in the data gaps are also underestimated. To deal with that problem, prior to the calculation of the variance-covariance matrix (section 5.4.2.), some modifications were directly made onto the signals of the ensemble of ocean mass solutions. The high frequency related signal component was added to the ensemble signals as follows:

- Application of a 1-year filter onto MASL data with prior removal of the annual and semi-annual components of the signal
- Calculation of the standard deviation of the difference between the initial and filtered MASL signal
- Stochastic addition with a normal (Gaussian) distribution of this residual standard deviation at the locations where the MASL is suffering from a lack of data

Note that this method is applied to all the data gaps on the full time period.

4.4.3.3. Comments/limitations

The spatial interpolation method applied is simple. More sophisticated algorithms could be applied to account for data gaps in the time series. Such methods based on the filter approach (e.g. Gaussian filter for spatial interpolation) are planned in future versions of the OHC change products. The impact on these improved algorithms is unknown at this time.

magellium

This document is property of Magellium. It cannot be reproduced,nor communicated without permission.

page 26/37

4.4.4. Calculation of regional Steric Sea Level change grids

4.4.4.1. Description

The objective is to calculate the regional (SL_{steric}) change grids from SL and MASL change grids.

The relationship between absolute sea level change (ΔSL), manometric sea level change (ΔMASL) and steric sea level change (SL_{steric}) is expressed by the sea level budget equation:

$$\Delta SL_{abs} = \Delta SL_{steric} + \Delta MASL \qquad \text{Eq. 8}$$

4.4.4.2. Mathematical statement

The (SL_{steric}) grids are obtained from the difference between SL and MASL grids at each time step. As SL and MASL grids have been preprocessed at same spatial and temporal resolution, the differences between grids is straightforward:

$$(\Delta SL_{steric})_{sat}(lon, lat, t) = (\Delta SL_{abs})(lon, lat, t) - \Delta MASL(lon, lat, t) \qquad \text{Eq. 9}$$

For each cell containing a default value in the SL and MASL change grids, a default value is assigned in the (SL_{steric}) change grids.

4.4.4.3. Comments/limitations

Other alternative methodologies are used to derive the steric sea level grids. They rely on in situ data instead of spatial data, mainly from temperature and salinity profiles provided by the Argo network. The advantages and inconvenients of such an approach is presented in Meyssignac et al. (2019).

Steric sea level is obtained by subtraction of signals. Some limitations related to this operation can be identified. The GIA datasets used to correct the gravimetry signals and the sea level from altimetry are not consistent (three different GIA corrections for the post-processing of gravimetry solutions and one solution for altimetry, see sections 3.2. and 4.4.2.1.). To date, the impact of such incoherency in the processing of data is expected to be low. However, a possible homogenisation of the pre-processing of altimetry and gravimetry datasets should solve this issue. Finally, the dynamical atmospheric correction based on MOG2D model (Carrère and Lyard, 2003) has been removed in altimetry processing whereas only the inverse barometer correction has been applied in gravimetry processing (Blazquez et al., 2018). The impact of this discrepancy must be studied and corrected if needed.

magellium

This document is property of Magellium. It cannot be reproduced,nor communicated without permission.

page 27/37

4.4.5. Calculation of regional OHC change grids

4.4.5.1. Description

The objective is to calculate the regional OHC change grids from satellite and $(SL_{steric})_{in\ situ}$ grids at the same spatial and temporal resolution. Once the IEEH variable is determined at regional scale, (SL_{steric}) change is translated to OHC change thanks to the IEEH at every timestep.

4.4.5.2. Mathematical statement

In order to get the ocean heat content change (in J/m²), we divide all grids of steric sea level changes (m) by the regional IEEH grid (m³.J^{-1}). According to the Eq. 2 given in section 2.2, the OHC change is expressed per unit of area (J.m^{-2}):

$$(OHC)_{sat} = (OHC)_{in\ situ} + \frac{(\Delta SL_{steric})_{sat} - (\Delta SL_{steric})_{in\ situ}}{(IEEH)_{in\ situ}}$$	Eq. 10

It results in monthly OHC change given on a 1°x1° resolution grid. For each cell containing a default value in the (SL_{steric}) or IEEH grids, a default value is assigned in the OHC grids.

5. Uncertainties calculation and propagation

5.1. Overview

In parallel to the product processing described in the previous section, the uncertainties are calculated and provided at each location for : SL, MASL, (SL_{steric}) and OHC change. The proposed approach consists in providing a variance-covariance matrix (Σ) of the errors for at every location in the Atlantic Ocean. Once the variance-covariance matrices are known, the trend uncertainties can be derived for any location and time spans of the time series. It is also possible to make it for any other indicators such as the mean, the acceleration or the magnitude of the annual signals at every location for instance. The method for deriving regional uncertainties is based on Prandi et al. (2021) for the absolute sea level trends and accelerations. This method does not take into account spatial correlations. As a matter of fact we will work with temporal correlations only.

magellium

This document is property of Magellium. It cannot be reproduced, nor communicated without permission.

page 28/37

The Figure 5 below describes main steps to propagate the uncertainties from the SL and MASL change grids until the OHC change grids. As we just consider time correlated errors, variance-covariance matrices are computed and propagated for every latitude and longitude couple.

The following subsections described the algorithms developed in detail.

For now, the variance-covariance matrices are computed at annual resolution.
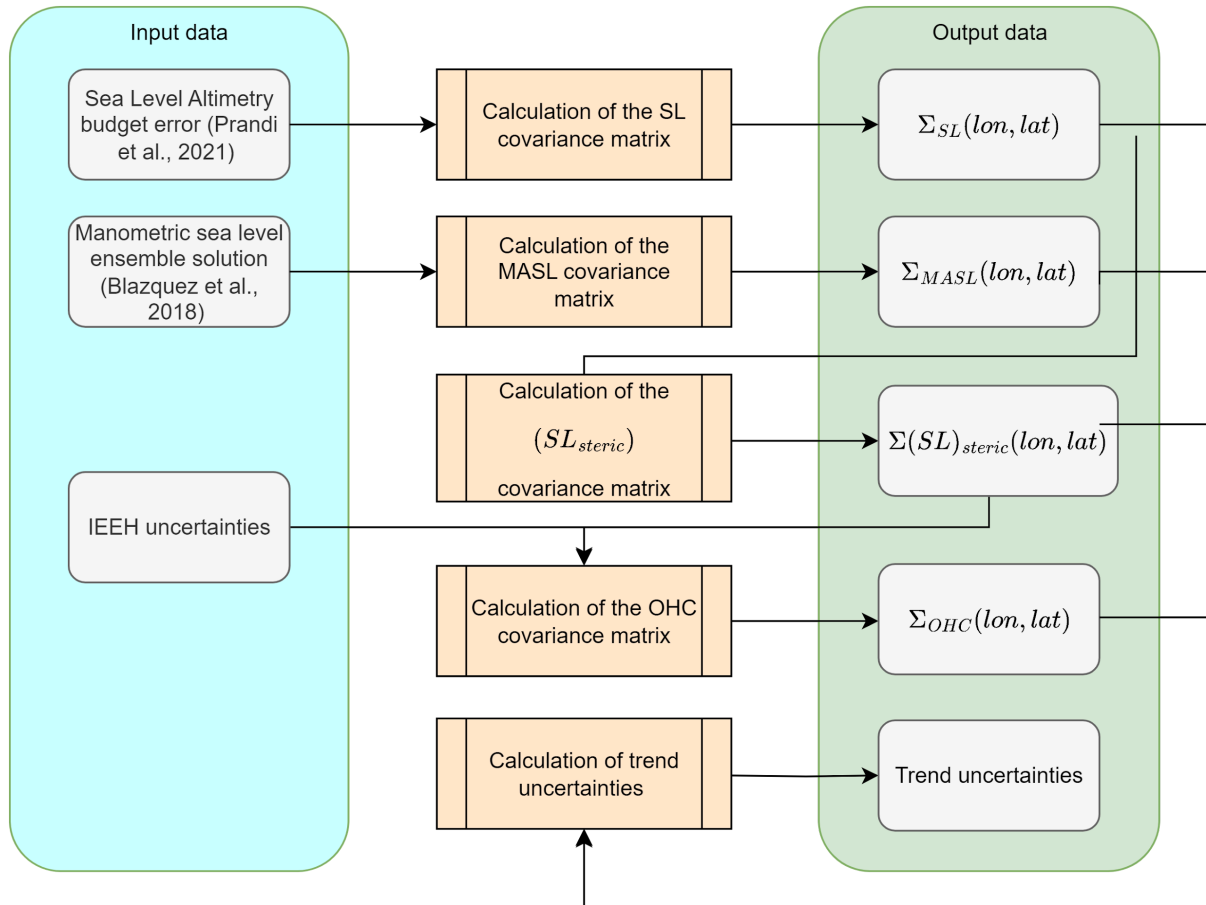
Figure 5: Uncertainty calculation and propagation chain

5.2. Input Data

The input data used are:
- the absolute sea level altimetry regional error budget given by (Prandi et al., 2021) and its associated variance-covariance matrix (displayed on table below),
- the ensemble of manometric sea level solutions provided by Blazquez et al. (2018) available in NetCDF format file on the LEGOS ftp site [Table 2, RD4].

This document is property of Magellium. It cannot be reproduced,nor communicated without permission.

page 29/37

- land mask (spatial resolution: 1° x 1°)
- the uncertainty of the Integrated Expansion Efficiency of Heat based on the dispersion of 11 in-situ solutions

Source of errors	Error category	Uncertainty level (at 1 σ)
High frequency errors: altimeter noise, geophysical corrections, orbits ...	Correlated errors (λ = 1 year)	σ = location dependent
Low frequency errors: wet tropospheric correction	Correlated errors (λ = 10 years)	σ = location dependent
Drift errors from the orbit determination	Drift error	δ = 0.33 mm/yr
Drift errors from the GIA correction	Drift error	δ = location dependent
inter-mission TP-a/TP-b and TP-b/J1 biases	Jump	Δ = 10 mm
inter-mission J1/J2 and J2/J3 biases	Jump	Δ = 6 mm

Table 4: Altimetry regional error budget given at 1-sigma

5.3. Output Data

Errors are characterised with the following variance-covariance matrices:

- $\Sigma_{SL}, \Sigma_{MASL}, \Sigma_{SL_{steric}}$ for the SL, MASL and (SL_{steric})
- Σ_{OHC} for the OHC

5.4. Retrieval methodology

5.4.1. Calculation of the SL covariance matrix

5.4.1.1. Description

For now, the error variance covariance matrix of SL (Σ_{SL}) is the one provided in (Prandi et al., 2021). It is deduced from the regional absolute sea level error budget described in Table 4 and computed at annual resolution. Thus, for each $(nlat, nlon)$ couple, a square matrix of variance-covariance is calculated with the dimensions $(ntime, ntime)$. The final object which contains all the variance-covariance matrices have the following dimensions: $\Sigma_{SL}(nlat, nlon, ntime, ntime)$

5.4.1.2. Mathematical statement

As it was assumed that all error sources shown in Table 4 are independent one to each other. The matrix is the sum of the individual variance-covariance matrices of each error source in the sea level error budget:

$$\Sigma_{SL} = \sum_{i=1}^{n} \Sigma_{Error_i}$$

Eq. 11

5.4.1.3. Comments/Limitations

This matrix is based on the current knowledge of altimetry measurement errors. As the altimetry record increases in length with new altimeter missions, the knowledge of the altimetry measurement also increases and the description of the errors improves. Consequently, the error variance-covariance matrix is expected to change and improve in the future – hopefully with a reduction of measurement uncertainty in new products.

It is also important to note that the error budget approach applied here to derive the variance-covariance matrix is conservative. In other words, absolute sea level from altimetry errors may be overestimated with respect to reality.

More information is given in (Prandi et al., 2021).

5.4.2. Calculation of the MASL covariance matrix

5.4.2.1. Description

The objective is to calculate the error variance-covariance matrix of the MASL grids (Σ_{MASL}) for the time period of the study (also at annual resolution by computing the annual mean of the ensemble). Σ_{MASL} is derived from an MASL ensemble deduced from the ensemble of ocean mass solutions provided by Blazquez et al. (2018), containing 60 GRACE(-FO) grids datasets.

magellium

This document is property of Magellium. It cannot be reproduced,nor communicated without permission.

page 31/37

5.4.2.2. Mathematical statement

The MASL data from GRACE(-FO) are available worldwide. Only ocean data is kept by applying the land mask. For each latitude and longitude of the MASL ensemble, the regional variance-covariance matrix is computed by using all the solutions of the ensemble for this given location.

The resulting MASL ensemble solutions contains n temporal vectors noted hereafter X_i for i=1 from 1 to n. The variance-covariance matrix (Σ_{MASL}) is the matrix whose entry is the covariance:

$$\Sigma_{MASL}(i,j) = cov(X_i, X_j) = E[(X_i - E[X_i])(X_j - E[X_j])]$$

where E is the mean operator.

5.4.2.3. Comments/Limitations

The ensemble provided by Blazquez et al. (2018) contains 60 solutions which is an important number of solutions to calculate Σ_{MASL}. However the mathematical formulation above assumes a normal distribution of the different MASL solutions. In practice, it is not fully the case. Thorough investigations must be performed to analyse the impact of this approximation.

In contrast to absolute sea level errors, the ensemble error approach applied here to derive a variance-covariance matrix could be considered as an optimistic view of the MASL error description. This means that MASL regional uncertainties could be underestimated.

5.4.3. Calculation of the Steric Sea Level covariance matrix

5.4.3.1. Description

The objective is to compute the variance-covariance matrix of the (SL_{steric}) errors ($\Sigma_{SL_{steric}}$). As (SL_{steric}) is obtained by calculating the differences between SL and MASL, $\Sigma_{SL_{steric}}$ is obtained by summing the variance-covariance matrices of the errors of SL and MASL. Indeed, since the errors of the two data sets are considered independent (see limitations section below) , the errors are additive.

5.4.3.2. Mathematical statement

$$\Sigma_{SL_{steric}} = \Sigma_{SL} + \Sigma_{MASL}$$

magellium

This document is property of Magellium. It cannot be reproduced,nor communicated without permission.

page 32/37

5.4.3.3. Comments/Limitations

The proposed method for calculating the (SL_{steric}) error variance-covariance matrix from the sum of the SL and MASL error variance-covariance matrix are based on two main assumptions :

- SL and MASL are assumed independent: this assumption is based on the fact that sensors are fully independent but in practice similar geophysical corrections are applied in their on-ground processing (e.g. GIA and ocean tide to calculate SL and MASL change) which can generate correlated errors not quantified to date. However we expect such error correlations to be negligible.
- Potential errors due to the collocation between the datasets (SL, MASL) have not been taken into account and the different sensors may not be able to observe the same signals due to their spatial and temporal coverage. Such studies must be performed in the future to evaluate this source of uncertainty.

5.4.4. Calculation of the OHC covariance matrix

5.4.4.1. Description

The objective is to calculate the variance-covariance matrix of the OHC change errors (Σ_{OHC}). The errors from (SL_{steric}) time series are propagated to the OHC change time series taking into account the relationship between the OHC and TSSL change via the regional integrated expansion efficiency of heat coefficient (ϵ or IEEH) and its uncertainty (e_ϵ). Σ_{OHC} is inferred from $\Sigma_{SL_{steric}}$ from the following relationship (see details in next subsection).

$$OHC(t, lat,\ lon)\ =\ \frac{(\Delta SL_{steric})\ (t,lat,lon) \pm e_{SSL}(t)}{\epsilon(t,lat,lon) \pm e_\epsilon}$$	Eq. 12

5.4.4.2. Mathematical statement

In case of two uncorrelated scalar variables a and b, with a respective uncertainty e_a and e_b, the error propagation division follows the ensuing relationship (Taylor, 1997, equation 3.8):

This document is property of Magellium. It cannot be reproduced, nor communicated without permission.

page 33/37

$$(e_{\frac{a}{b}})^2 \;=\; \left(\frac{1}{b}\right)^2 * \left[e_a^{\;2} \;+\; \left(e_b * \frac{a}{b}\right)^2 \right]$$

Eq. 13

In our case:

- a= (SL_{steric})(t, lat,lon) and ϵ_a is e_{SSL}(t, lat, lon)
- b= IEEH (noted ϵ) and ϵ_b is given by e_ϵ
- $\dfrac{a}{b} \;=\; \dfrac{(\Delta SL_{steric})(t, lat, lon)}{IEEH(t, lat, lon)} \;=\; \Delta OHC(t,\ lat,\ lon)$

Thus with these notations, the first equation becomes:

$$(e_{\Delta OHC(t, lat, lon)})^2 \;=\; \frac{1}{\epsilon(t,lat,lon)^2} * (e_{(\Delta SL_{steric})(t, lat, lon)})^2 \;+\; \left(\frac{e_\epsilon}{\epsilon(t,lat,lon)}\right)^2 * (\Delta OHC(t,\ lat,\ lon))$$

Eq. 14

which can be written in matricial notation with the variance-covariance matrices Σ_{OHC} and $\Sigma_{SL_{steric}}$ (containing the uncertainties $e_{OHC}^{\;2}$ and $e_{SL_{steric}}^{\;2}$ respectively) as follows:

$$\Sigma_{\Delta OHC(lat,lon)} \;=\; \frac{1}{\epsilon(lat,lon)^2}\Sigma_{(\Delta SL_{steric})(lat,lon)} \;+\; \left(\frac{e_\epsilon}{\epsilon(lat,lon)}\right)^2 \Delta OHC(lat, lon) * \Delta OHC(lat, lon)^T$$

Eq. 15

5.4.4.3. Uncertainties of the regional IEEH

As the IEEH is not an intensive parameter (i.e. it can not be averaged from regional scale to global scale), it is not suitable to take the uncertainty associated with the global IEEH (Marti et al., 2022b) at regional scales.

To estimate uncertainty at regional scale of the IEEH, an ensemble of several IEEH estimates based on 9 different centers SIO, EN4, JAMSTEC, IAP, IPRC, ISAS (Cheng et al., 2017; Gaillard et al., 2016; Good et al., 2013; Hosoda et al., 2010; Roemmich et al., 2009) have been computed. Then an estimation of the standard deviation of these products is computed and used as an estimate of the uncertainty of the IEEH (Figure 6).
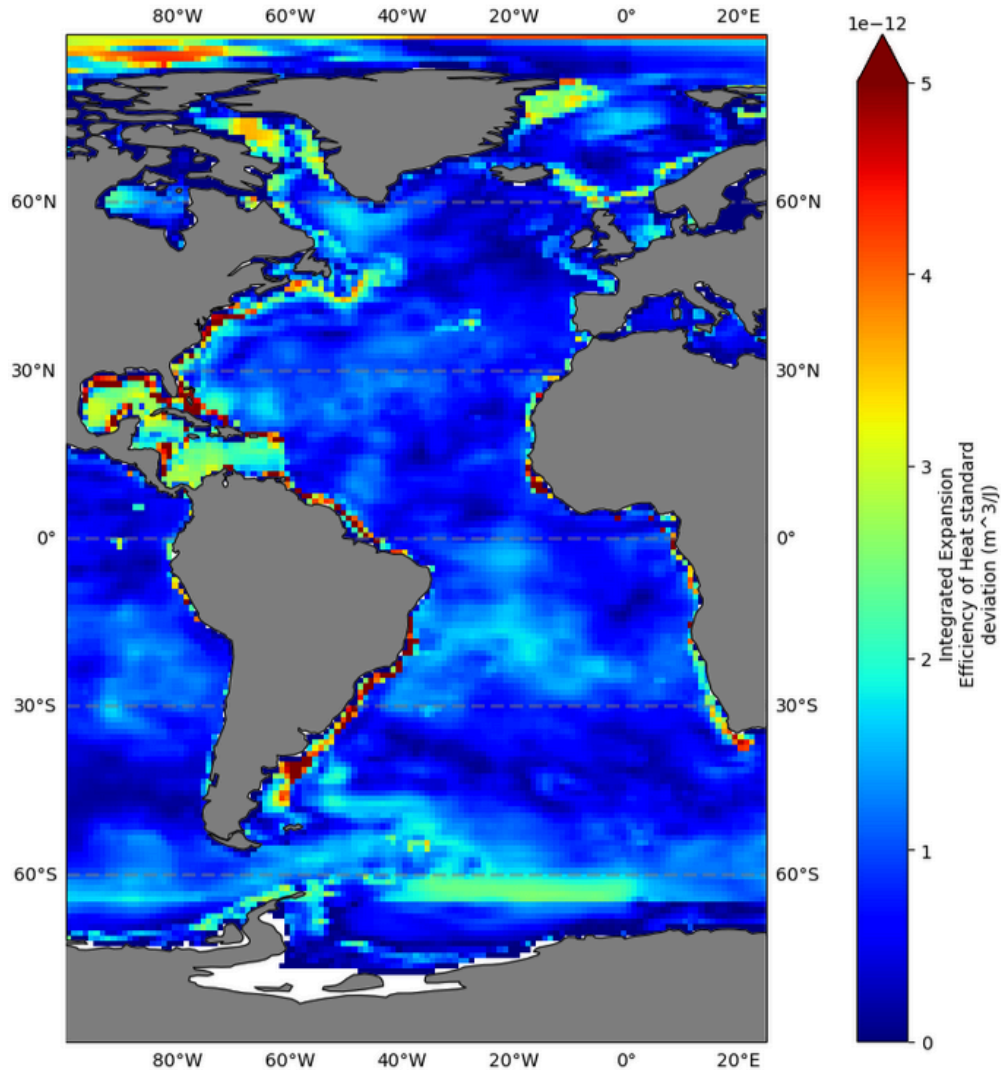
Figure 6: Uncertainty on the IEEH coefficient

5.4.4.4. Comments/Limitations

In this formalism, it has been decided to use the uncertainty of the global IEEH rather than the uncertainty of local IEEH.

The mathematical formalism proposed for the propagation of errors from the (SL_{steric}) change to the OHC change shows that the errors of the OHC change depend both on the uncertainty of the value of the IEEH coefficient and on the value of the coefficient itself. When analysing the impact of changing this coefficient and its uncertainty (from Levitus et al., 2012/Kuhlbrodt and Gregory, 2012 to Marti et al., 2022), we found that this significantly reduced OHC change uncertainties.

Moreover, uncertainties from the $(SL_{steric})_{in\ situ}$ and $(OHC)_{in\ situ}$ are not taken into account in the uncertainty propagation. Investigations are on-going to estimate them.

magellium

This document is property of Magellium. It cannot be reproduced,nor communicated without permission.

page 35/37

5.4.5. Calculation of trend uncertainties

5.4.5.1. Description

The objective is to calculate the trend uncertainty, adjusting a polynomial of degree 1 by an ordinary least square (OLS) method taking into account the error variance-covariance matrix for the calculation of the uncertainty.

5.4.5.2. Mathematical statement

The ordinary least square (OLS) regression method is used in this study. The estimator of β with the OLS approach is noted:

$$\hat{\beta} \sim (X^t X)^{-1} X^t y \qquad \text{Eq. 16}$$

where y is the vector containing the observations (e.g. SL change, OHC change, … at each location) and X the vector containing the dates of the observations.

The uncertainty in the trend estimates takes into account the correlated errors of the observations (y). So, the error is integrated into the trend uncertainty estimation. Taking into account the variance-covariance matrix (Σ) , the estimator of β becomes:

$$\hat{\beta} = N(\beta, (X^t X)^{-1} (X^t \Sigma X)(X^t X)^{-1}) \qquad \text{Eq. 17}$$

5.4.5.3. Comments/Limitations

As we just consider time correlated errors and not the spatial errors, the inversion of the matrix is done on the $nlat * nlon$ square matrices of dimension $(ntime, ntime)$.

The proposed approach is also applicable for any other adjusted variables. For instance, the acceleration of the time series can be calculated from the adjustment of a polynomial of degree 2 $(a_0 + a_1 X + a_2 X^2)$ where the acceleration (a) is given by $a = 2a_2$. The uncertainty acceleration is calculated applying the same mathematical formalism described previously for the trend.

.